14

Rudder Roll Stabilisation of Ships

Contributed by Tristan Perez

14.1 Overview

In this chapter, we present a case study of control system design for rudder-based stabilisers of ships using RHC. The rudder's main function is to correct the heading of a ship; however, depending on the type of ship, the rudder may also be used to produce, or correct, roll motion. Rudder roll stabilisation consists of using rudder-induced roll motion to reduce the roll motion induced by waves. When this technique is employed, an automatic control system is necessary to provide the rudder command based on measurements of ship motion. The RHC formulation provides a unified framework to address many of the difficulties associated with this control system design problem.

14.2 Ship Roll Stabilisation

The success or failure of a ship's mission (fishing, landing a helicopter on deck, serving meals during transit, and so on) is judged by comparing the ship's performance indices with levels that are deemed satisfactory for the particular mission, type of ship and sea environment considered. To accomplish missions successfully, and to improve the performance, marine vehicles are often equipped with sophisticated devices and control systems. Amongst the many different control systems encountered on board a marine vehicle, there is often the so-called *roll stabilising system*, or simply *stabiliser*, whose function is to reduce undesirable roll motion.

Reduced roll motion is important for it can affect the performance of the ship, as indicated in the following considerations.

- Transverse accelerations that occur due to roll interrupt tasks performed by the crew. This increases the amount of time required to complete a mission.
- Roll accelerations may produce cargo damage, for example, on soft loads such as fruit.
- Roll motion increases hull resistance.
- Large roll angles limit crew capability to handle equipment on board, and/or to launch and recover systems.

Several type of stabilisers and stabilisation techniques have been developed and are commonly used: bilge keels, water tanks, fins and rudder (see Sellars and Martin (1992) for a description and benefits of each of these stabilisers).

Amongst the different types of stabilisers, rudder-based stabilisation is a very attractive technique. The reasons for this are that almost every ship has a rudder (thus no extra equipment may be necessary), and also this technique can be used in conjunction with other stabilisers (such as water tanks and fins) to improve performance under various conditions. In this chapter, we will focus on the control system design of rudder-based stabilisers. As we shall see, this design problem is far from trivial.

14.3 A Challenging Control Problem

Using the rudder for simultaneous course keeping and roll reduction is not a simple task. The ability to accomplish this depends on the dynamic characteristics of the ship, and also on the control strategy used to command the rudder. The design of such a control strategy must then be performed so as to best deal with the following issues:

- **Underactuated System**. One control action (rudder force) achieves two control objectives: *roll reduction* and *low heading (yaw) interference*. A key fact that must be understood for the successful application of this technique is that the dynamics associated with the rudder-induced roll motion are faster than the dynamics associated with the rudder-induced yaw motion. This phenomenon depends on the shape of the hull and the location of the rudder and the centre of gravity of the ship. The difference in dynamic response between roll and yaw is characterised by the location of a nonminimum phase zero [NMP] associated with the rudder to roll response. The closer the NMP zero is to the imaginary axis, the faster the roll response to the rudder will be with respect to the response in yaw; and, thus, the better the potential for successful application of rudder roll stabilisation (Roberts 1993). Nevertheless, this effect of the NMP zero will not, per se, guarantee good performance in all conditions; see Perez (2003) for details.

- **Uncertainty**. There are three sources of uncertainty associated with the control problem. First, there is incomplete state information available to implement the control law. Although, complete measurement of the state is possible, the necessary sensors can be very expensive. Second, there are disturbances from the environment (wave-induced motion) that, in principle, cannot be known a priori. Third, in the case of model-based control (such as RHC), there is uncertainty associated with the accuracy of the model.
- **Disturbance Rejection with a Nonminimum Phase System**. As already mentioned, the response of roll due to rudder action presents nonminimum phase dynamics. This imposes fundamental limitations and trade-offs regarding disturbance rejection and achievable roll reduction in different *sailing conditions* (ship speed and heading relative to the waves). The energy of the disturbance shifts in frequency according to the sea state and sailing conditions. Because these changes can be significant, roll amplification can be induced if the controller is not adapted to the changes in the disturbance characteristics (see, for example, Blanke, Adrian, Larsen and Bentsen 2000, Perez 2003). This is a consequence of reducing the sensitivity close to the frequency of the NMP zero.
- **Input constraints**. The rudder action demanded by the controller should satisfy *rate* and *magnitude* constraints. Rate constraints are associated with safety and reliability. By imposing rate constraints on the rudder command, we ensure an adequate lifespan of the hydraulic actuators and avoid their saturation. However, this produces time delays that could lead to stability problems. Magnitude constraints are associated with performance and economy. Large rudder angles induce flow separation (loss of actuation and poor performance), and a significant increase in drag (resistance). Also, it is desirable to reduce the maximum rudder action at higher speeds to reduce the mechanical loads on the rudder and the steering machinery.
- **Output constraints**. Since the rudder affects the ship heading, it may be necessary to include constraints on the maximum heading deviations allowed when the rudder is used to reduce roll.
- **Unstable plant**. The response of yaw to rudder action is marginally unstable: there is an integrator. Indeed, if the rudder is offset from its central position with a step-like command, there will be a ramp-like increase in the heading angle. Some vessels are even directionally unstable, requiring permanent rudder offset to keep a heading.

Based on the above considerations, it is evident that the problem of rudder roll stabilisation of ships is a challenging one and, as such, the chosen control strategy plays an important role in achieving high performance. In what follows, we will further describe the different effects that give rise to the issues mentioned above, define the performance criteria and carry out the design.

14.4 Ship Motion Description and Modelling for Control

The motion of a marine vehicle can be considered in six degrees of freedom. The motion components are resolved into translation components in three directions: *surge*, *sway* and *heave*, and rotation components about three axis: *roll*, *pitch* and *yaw*. Table 14.1 shows the notation used to describe the different motion components.

translation	surge	sway	heave
position	x	y	z
linear rate	u	v	w

rotation	roll	pitch	yaw
angle	ϕ	θ	ψ
angular rate	p	q	r

Table 14.1. Adopted nomenclature for the description of ship motion.

To describe the motion of a vehicle, two reference frames are considered: an *inertial* frame and a *body-fixed* frame. Figure 14.1 shows the two reference frames together with the variables often expressed relative to these frames. This figure also indicates the adopted positive convention.

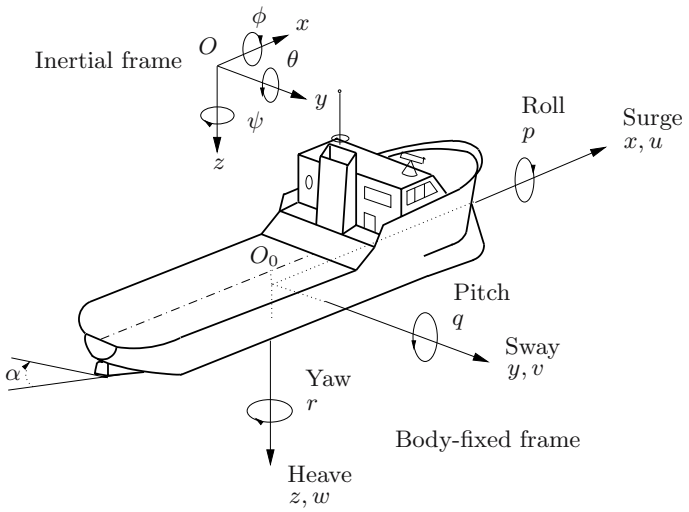

Figure 14.1. Notation, reference frames and sign conventions for ship motion description.

For marine vehicles position and orientation are described relative to the inertial reference frame, whilst linear and angular velocities are expressed in the body-fixed frame. This choice is convenient since some of these magnitudes are measured on board, and thus, relative to the body-fixed frame. In addition,

by choosing the appropriate location of the body-fixed frame, the resulting equations of motion that describe the dynamic behaviour of the vessel are simplified—see Fossen (1994) for details.

A convenient abstraction to obtain a mathematical model that captures the different effects that give rise to ship motion, is to separate the motion due to control action (rudder motion) from the motion due to the waves. This abstraction results in two models that can be combined using superposition (Faltinsen 1990).

The first part of the model can be obtained using Newton's laws. This approach yields a nonlinear model that describes the motion components in terms of the forces and moments acting on the hull (Fossen 1994). By linearising this model and incorporating a linear approximation of the forces and moments generated by the rudder, we can obtain a linear state space model that describes the ship response due to the rudder (control) action. A discrete time version of this model can be expressed as

$$x_{k+1}^c = A_c x_k^c + B_c u_k, \tag{14.1}$$

where the state x_k^c and control u_k, are given by (see Figure 14.1 and Table 14.1)

$$x_k^c = \left[v_k^c \; p_k^c \; r_k^c \; \phi_k^c \; \psi_k^c\right]^{\mathrm{T}} \quad \text{and} \quad u_k = \alpha_k, \tag{14.2}$$

with α_k being the current rudder angle.

For the particular motion control problem being considered, it is a common practice to decouple the vertical motion components of pitch and heave and to consider a constant forward speed. Hence, the surge equation can also be decoupled leaving a model that captures the couplings between roll, sway and yaw, that is, the state indicated in (14.2).

The parameters of the model (14.1), the values of the entries of the matrices A_c and B_c, will vary with the forward speed of the vessel. However, this variation is such that constant values can be considered for different speed ranges; usually close to the nominal speed of the vessel. Because of this, system identification techniques and data collected from tests in calm water can be used to estimate the parameters for different speed ranges; see, for example, Zhou, Cherchas and Calisal (1994). The different sets of parameters can then be used in a gain scheduling-like approach to update the model. This helps to minimise model uncertainty.

The second part of the model incorporates the motion induced by the waves. The sea surface elevation can be described in stochastic terms by its power spectral density; or, simply, *sea spectrum*. The ship motion induced by the waves can be interpreted as a filtering process made by the ship's hull, which has a selected response to certain frequencies and attenuates others. The frequency response of the hull due to wave excitation is called the *ship response operator*. The total effect can be incorporated into our model as a coloured noise output disturbance. The roll motion induced by the waves will thus be modelled with a shaping filter:

$$\begin{aligned} x_{k+1}^w &= A_w x_k^w + w_k, \\ y_k^w &= x_k^w + v_k, \end{aligned} \tag{14.3}$$

where $x^w = [p^w \quad \phi^w]^{\mathrm{T}}$, and w_k and v_k are sequences of i.i.d. Gaussian vectors with appropriate dimensions.

For a given hull shape, the filtering characteristics of the hull depend on the forward speed of the ship U, and the heading angle relative to the waves: the *encounter angle* χ, which is defined as indicated in Figure 14.2. The variations in the characteristics of the motion response due to speed and encounter angle are the consequence of a Doppler-like effect. Indeed, if the ship is moving with a forward speed, the wave frequency observed from the ship is, in general, different from that observed from a fixed zero-speed reference frame. The frequency observed from the ship is called the *encounter frequency* ω_e. Expression (14.4) shows the relationship between the wave frequency ω_w (observed from a fixed-reference frame), and the encounter frequency:

$$\omega_e = \omega_w - \frac{\omega_w^2 U}{g} \cos\chi. \tag{14.4}$$

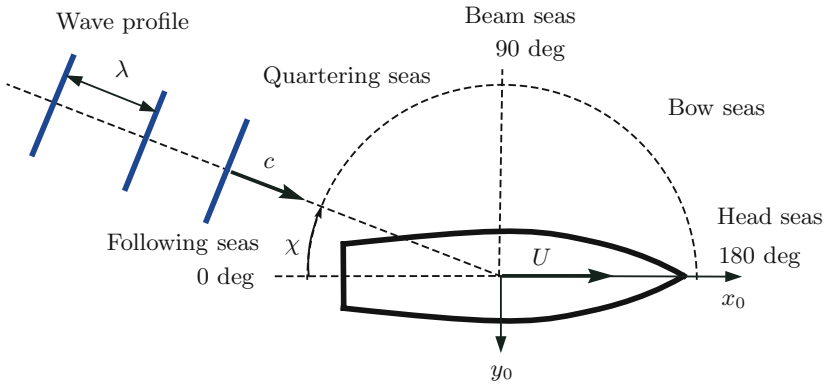

Figure 14.2. Encounter angle definition and usual denomination for sailing conditions.

The encounter effect produces significant variations in the motion response of the ship even for the same sea state, hereby defined by the sea spectrum. Consequently, the values of the parameters of the model (14.3) should be

updated for changes in different sea states and sailing conditions. We will address this point in a latter section.

The complete state space model can then be represented via state augmentation as

$$\begin{aligned} x_{k+1} &= Ax_k + Bu_k + Jw_k, \\ y_k &= Cx_k + n_k, \end{aligned}$$

where $x^{\mathrm{T}} = [x_k^c \quad x_k^w]$. The following measurements are assumed available to implement the control:

$$\begin{aligned} y_k &= \begin{bmatrix} p_k & r_k & \phi_k & \psi_k \end{bmatrix}^{\mathrm{T}} + n_k \\ &= \begin{bmatrix} (p_k^c + p_k^w) & r_k^f & (\phi_k^c + \phi_k^w) & \psi_k^f \end{bmatrix}^{\mathrm{T}} + n_k, \end{aligned} \tag{14.5}$$

where, n_k is noise introduced by the sensors, and r_k^f and ψ_k^f are the filtered yaw rate and yaw angle respectively.

The ramifications of an output disturbance model shall be evident when we estimate the parameters of the disturbance part of the model. Note also that we have only considered the wave disturbance affecting the roll angle and the roll rate but not the yaw. The reason for this is that, in conventional autopilot design, the yaw is filtered and only low frequency yaw motion is corrected. This is done to avoid the autopilot making corrections to account for the first-order (sinusoidal) wave-induced yaw motion. Therefore, in the problem we are assuming that the yaw is measured after the yaw wave filter; see Fossen (1994) and Blanke et al. (2000) for details.

14.5 Control Problem Definition

The basic control objectives for the particular motion control problem being addressed here are as follows:

(i) minimise the roll motion, which includes roll angle and accelerations;
(ii) produce low interference with yaw;
(iii) satisfy input constraints.

In a discrete time framework, all the above objectives are captured in the following optimisation problem.

Definition 14.5.1 (Output Feedback Control Problem with Input Constraints) *Find the feedback control command $u_k = \mathcal{K}(y_k)$ that minimises the objective function*

$$V = \lim_{N\to\infty} \frac{1}{N} \mathbf{E}\left\{ \sum_{k=0}^{N} y_k^{\mathrm{T}} Q y_k + (y_{k+1} - y_k)^{\mathrm{T}} S (y_{k+1} - y_k) + u_k^{\mathrm{T}} R u_k \right\} \tag{14.6}$$

subject to the system equations

$$x_{k+1} = Ax_k + Bu_k + Jw_k,$$
$$y_k = Cx_k + n_k,$$

and the input constraints

$$|u_k| \leq u_{max} \qquad \text{and} \qquad |u_{k+1} - u_k| \leq \delta u_{max},$$

with y_k *given in* (14.5). ∘

Choosing the matrices Q and S as:

$$Q = \text{diag}\{0, Q_p, 0, Q_\phi, Q_\psi\},$$
$$S = \text{diag}\{0, S_p, 0, 0, 0\},$$

the objective function (14.6) becomes (assuming no sensor noise)

$$V = \lim_{N\to\infty} \frac{1}{N} \mathbf{E}\Big\{ \sum_{k=0}^{N} \left[Q_p p_k^2 + Q_\phi \phi_k^2 + S_p (p_{k+1} - p_k)^2 \right] + Q_\psi \psi_k^2 + R\alpha_k^2 \Big\}, \tag{14.7}$$

which can be interpreted as

$$V \propto Q_p \, \mathbf{var}[p] + Q_\phi \, \mathbf{var}[\phi] + S_p \, \mathbf{var}[\dot{p}] + Q_\psi \, \mathbf{var}[\psi] + R \, \mathbf{var}[\alpha].$$

The objective function (14.7) is a discrete time version of the objective function proposed by van Amerongen, van der Klught and Pieffers (1987). The function (14.7), however, incorporates an extra term that weights the roll accelerations via the difference $p_{k+1} - p_k$. The reason for incorporating this extra term is that both roll angle and roll acceleration affect the performance of the ship; these are directly related to the criteria often used to evaluate ship performance in the marine environment (see Lloyd 1989, Graham 1990).

We next show how the above problem can be cast in the RHC framework.

14.6 A Receding Horizon Control Solution

As discussed in Chapter 12, the problem defined above is not easy to solve due to the presence of constraints.

We will approximate its solution using the certainty equivalent solution of an associated finite horizon problem, together with a receding horizon implementation.

In this context, we define the following associated finite horizon problem.

Definition 14.6.1 (Finite Horizon Optimal Control Problem) *Given the initial condition* $\check{x}_0$*, we seek the sequence of control moves*

$$\{\check{u}_0^{\text{OPT}}(\check{x}_0), \ldots, \check{u}_{N-1}^{\text{OPT}}(\check{x}_0)\} \tag{14.8}$$

that minimises the objective function

$$V_N \triangleq \frac{1}{2}\check{x}_N^{\mathrm{T}}\check{P}\check{x}_N + \sum_{j=0}^{N-1}\frac{1}{2}(\check{x}_j^{\mathrm{T}}\check{Q}\check{x}_j + \check{u}_j^{\mathrm{T}}\check{R}\check{u}_j + \check{u}_j^{\mathrm{T}}\check{T}\check{x}_j + \check{x}_j^{\mathrm{T}}\check{T}^{\mathrm{T}}\check{u}_j), \tag{14.9}$$

subject to

$$\begin{aligned}\check{x}_{j+1} &= A\check{x}_j + B\check{u}_j,\\ \check{y}_j &= C\check{x}_j,\end{aligned} \tag{14.10}$$

and the constraints

$$|\check{u}_j| \leq u_{max} \qquad \text{and} \qquad |\check{u}_{j+1} - \check{u}_j| \leq \delta|u_{max}.$$

The augmented state $\check{x}$ *in* (14.10) *is given by*

$$\check{x} = \begin{bmatrix}\check{v}^c & \check{p}^c & \check{r}^c & \check{\phi}^c & \check{\psi}^c & \check{\phi}^w & \check{p}^w\end{bmatrix}^{\mathrm{T}}.$$

NB. The notation $\check{x}$ *is used here to distinguish the predicted state (predicted using the model* (14.10)*) from the true state* x*.*

The matrices in the objective function are

$$\begin{aligned}\check{Q} &= (A-I)^{\mathrm{T}}(C^{\mathrm{T}}SC)(A-I) + C^{\mathrm{T}}QC,\\ \check{R} &= B^{\mathrm{T}}(C^{\mathrm{T}}SC)B + R,\\ \check{T} &= B^{\mathrm{T}}(C^{\mathrm{T}}SC)(A-I).\end{aligned}$$

The matrices Q*,* S *and* R *are the parameters defining the objective function* (14.6)*, and the matrices* A*,* B *describing the augmented system are*

$$A = \begin{bmatrix}A_c & 0\\ 0 & A_w\end{bmatrix}, \quad B = \begin{bmatrix}B_c\\ 0\end{bmatrix}, \tag{14.11}$$

where the zeros denote zero matrices of appropriate dimensions. The matrix $\check{P}$ *in* (14.9) *is taken as the solution of the following discrete time algebraic Riccati equation:*

$$\check{P} = A^{\mathrm{T}}\check{P}A + \check{Q} - K^{\mathrm{T}}\bar{R}K.$$

with $K = \bar{R}^{-1}B^{\mathrm{T}}\check{P}A$ *and* $\bar{R} = \check{R} + B^{\mathrm{T}}\check{P}B$*.* ∘

The cross terms in the objective function (14.9), which were not considered in the earlier RHC formulation given in Chapter 5 (see (5.9)), appear due to the terms in the objective function penalising the difference $p_{k+1} - p_k$. These cross terms only affect the matrices that define the associated quadratic program [QP]. The QP solution of the above problem is given by (see Section 5.3 in Chapter 5)

$$\mathbf{u}^{\mathrm{OPT}}(\check{x}_0) = \underset{L\mathbf{u}\leq W}{\arg\min}\ \frac{1}{2}\mathbf{u}^{\mathrm{T}}(H_1 + H_2)\mathbf{u} + \mathbf{u}^{\mathrm{T}}(F_1 + F_2)\check{x}_0, \tag{14.12}$$

where

$$H_1 = \Gamma^{\mathrm{T}}\mathbf{Q}\Gamma + \mathbf{R}, \qquad H_2 = \mathbf{T}\bar{\Gamma} + \bar{\Gamma}^{\mathrm{T}}\mathbf{T}^{\mathrm{T}},$$
$$F_1 = \Gamma^{\mathrm{T}}\mathbf{Q}\Omega, \qquad F_2 = \mathbf{T}\bar{\Omega},$$

$$\mathbf{Q} = \mathrm{diag}\{\check{Q}, \ldots, \check{Q}, \check{P}\},$$
$$\mathbf{R} = \mathrm{diag}\{\check{R}, \ldots, \check{R}\},$$
$$\mathbf{T} = \mathrm{diag}\{\check{T}, \ldots, \check{T}\},$$

and

$$\Omega = \begin{bmatrix} A \\ A^2 \\ \vdots \\ A^N \end{bmatrix}, \qquad \bar{\Omega} = \begin{bmatrix} I \\ A \\ \vdots \\ A^{N-1} \end{bmatrix},$$

$$\Gamma = \begin{bmatrix} B & 0 & \cdots & 0 \\ AB & B & \cdots & 0 \\ \vdots & \vdots & \ddots & \vdots \\ A^{N-1}B & A^{N-2}B & \cdots & B \end{bmatrix} \quad \bar{\Gamma} = \begin{bmatrix} 0 & 0 & \cdots & 0 \\ B & 0 & \cdots & 0 \\ \vdots & \vdots & \ddots & \vdots \\ A^{N-2}B & A^{N-3}B & \cdots & 0 \end{bmatrix}.$$

The matrices L and W that define the constraint set in (14.12) are given by (see Section 5.3.2 in Chapter 5)

$$L = \begin{bmatrix} I \\ E \\ -I \\ -E \end{bmatrix}; \quad W = \begin{bmatrix} \bar{M}_{\mathrm{mag}} \\ \bar{M}_{\mathrm{rate}} \\ \bar{M}_{\mathrm{mag}} \\ \bar{M}_{\mathrm{rate}} \end{bmatrix}$$

where I is the $N \times N$ identity matrix and E is the $N \times N$ matrix

$$E = \begin{bmatrix} 1 & \cdots & & 0 \\ -1 & 1 & & 0 \\ \vdots & \ddots & \ddots & \vdots \\ 0 & \cdots & -1 & 1 \end{bmatrix},$$

and

$$\bar{M}_{\mathrm{mag}} = \begin{bmatrix} u_{\max} \\ \vdots \\ u_{\max} \end{bmatrix}; \qquad \bar{M}_{\mathrm{rate}} = \begin{bmatrix} u_{-1} + \delta u_{\max} \\ \delta u_{\max} \\ \vdots \\ \delta u_{\max} \end{bmatrix}.$$

The above problem is be solved on line, and the implicit receding horizon feedback control law is implemented, that is,

$$u_k = \mathcal{K}_N(\check{x}_0(y_k)) = \check{u}_0^{\mathrm{OPT}}(\check{x}_0(y_k)),$$

the first element of the optimal sequence (14.8).

Using the certainty equivalence principle as described in Chapter 12 the initial condition for solving the above problem is provided by a Kalman filter (see Theorem 9.6.2 in Chapter 9). That is, at each step k we take $\check{x}_0 = \hat{x}_{k|k}$, where:

Prediction:

$$\begin{aligned} \hat{x}_{k|k-1} &= A\hat{x}_{k-1|k-1} + Bu_{k-1}, \\ \Sigma_{k|k-1} &= A\Sigma_{k-1|k-1}A^{\mathrm{T}} + R_w. \end{aligned} \tag{14.13}$$

Measurement update:

$$\begin{aligned} L_k &= \Sigma_{k|k-1}C^{\mathrm{T}}(C\Sigma_{k|k-1}C^{\mathrm{T}} + R_v)^{-1}, \\ \hat{x}_{k|k} &= \hat{x}_{k|k-1} + L_k(y_k - C\hat{x}_{k|k-1}), \\ \Sigma_{k|k} &= (I_n - L_kC)\Sigma_{k|k-1}, \end{aligned} \tag{14.14}$$

The predictions $\check{x}_j$ used in the finite horizon problem (see (14.10)) are then j-step predictions given the measurement y_k at the time instant k, that is,

$$\check{x}_j = \hat{x}_{k+j|k}.$$

To summarise the proposed control strategy, the following steps are envisaged at each sampling instant:

(i) Take measurements, that is, obtain y_k (see (14.5)) and the previous control action u_{k-1}.
(ii) Update the state prediction (14.13) and estimate the state $\hat{x}_{k|k}$ using (14.14) and the measured output.
(iii) Using u_{k-1} and the initial condition $\check{x}_0 = \hat{x}_{k|k}$ solve the QP (14.12) to obtain the sequence of controls (14.8).
(iv) Update the control command $u_k^c = \check{u}_0^{\mathrm{OPT}}(\check{x}_0)$.

Thus far, we have defined the control and the estimation problem. The only missing element of the proposed strategy is a method to update the parameters of the model that describes the wave-induced motion, that is, the matrix A^w in (14.11).

14.7 Disturbance Model Parameter Estimation

The solution proposed in the previous section assumes that a model is available to predict the output disturbance; namely, (14.3). Here, we present a simple approach to estimate the parameters based on the control scheme shown in Figure 14.3. If the stabiliser control loop is open (see Figure 14.3)—that is,

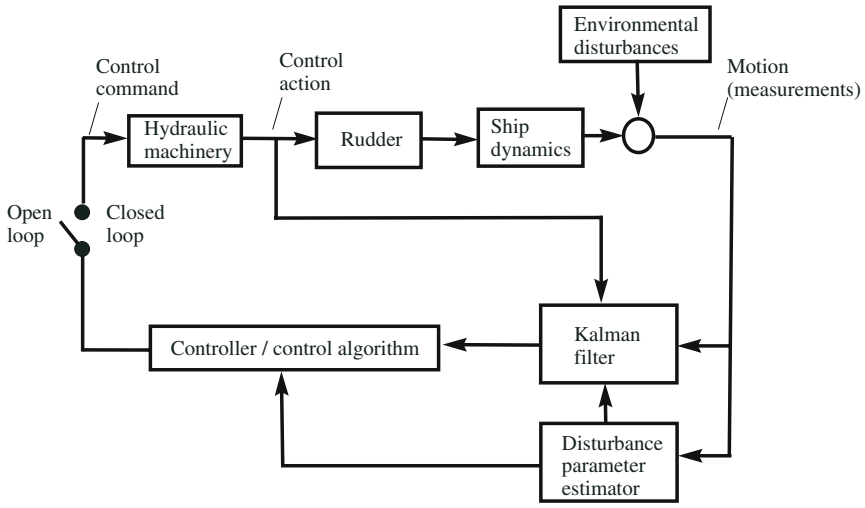

Figure 14.3. Block diagram of the control system architecture used for design.

the rudder is kept to zero angle, and only minor corrections are applied to the rudder to keep the course—we can then use the roll angle and roll rate measurements to estimate the parameters of a second order shaping filter. Under these conditions, the measurements coincide with the state of the following shaping filter:

$$\begin{bmatrix} \phi_{k+1}^w \\ p_{k+1}^w \end{bmatrix} = \begin{bmatrix} \theta_{11} & \theta_{12} \\ \theta_{21} & \theta_{22} \end{bmatrix} \begin{bmatrix} \phi_k^w \\ p_k^w \end{bmatrix} + \begin{bmatrix} w_k^\phi \\ w_k^p \end{bmatrix}.$$

By defining the vector

$$\theta_k = \begin{bmatrix} \theta_{11}(k) & \theta_{12}(k) & \theta_{21}(k) & \theta_{22}(k) \end{bmatrix}^{\mathrm{T}},$$

we can express the available measurements as

$$\begin{aligned} \theta_{k+1} &= \theta_k + \theta_{wk}, \\ \begin{bmatrix} \phi_k^w \\ p_k^w \end{bmatrix} &= \begin{bmatrix} \phi_{k-1}^w & p_{k-1}^w & 0 & 0 \\ 0 & 0 & \phi_{k-1}^w & p_{k-1}^w \end{bmatrix} \theta_k + v_k. \end{aligned} \tag{14.15}$$

The system (14.15) is in a form that we can apply a Kalman filter (see (14.14) and (14.13)) to estimate $\hat{\theta}_{k|k}$ from the measurements ϕ_k^w and p_k^w. The variable θ_{wk} represents a small random variable that accounts for unmodelled dynamics, so the Kalman filter does not assume a perfect model and eventually stops incorporating the information provided by the measurements. This method is a recursive implementation of the least-squares estimation method; see, for example, Goodwin and Sin (1984).

To assess the proposed method to estimate the parameters of the filter and the quality of the prediction using the above model, a series of simulations were performed generating the roll angle and roll rate as a sum of regular components using parameters corresponding to different sea states and sailing conditions.

The parameters to describe the sea state that were used are the average wave period T and the significant wave height H_s (average of the highest one third of the wave heights). These parameters are used in the International Towing Tank Conference (ITTC, 1952, 1957) recommended model for the wave power spectral density, commonly termed *ITTC spectrum* in the marine literature (Lloyd 1989):

$$\mathbf{S}_{\zeta\zeta}(\omega_w) = \frac{172.75 H_s^2}{T^4 \omega_w^5} \exp\left\{\frac{-691}{T^4 \omega_w^4}\right\} \qquad (\mathrm{m}^2\mathrm{sec/rad}). \tag{14.16}$$

The above sea state description is combined with the ship roll response operator to obtain the roll power spectral density and then simulate the time series used to estimate the parameters. The process for obtaining the ship roll power spectral density is indicated via an example in Figure 14.4. The first two plots

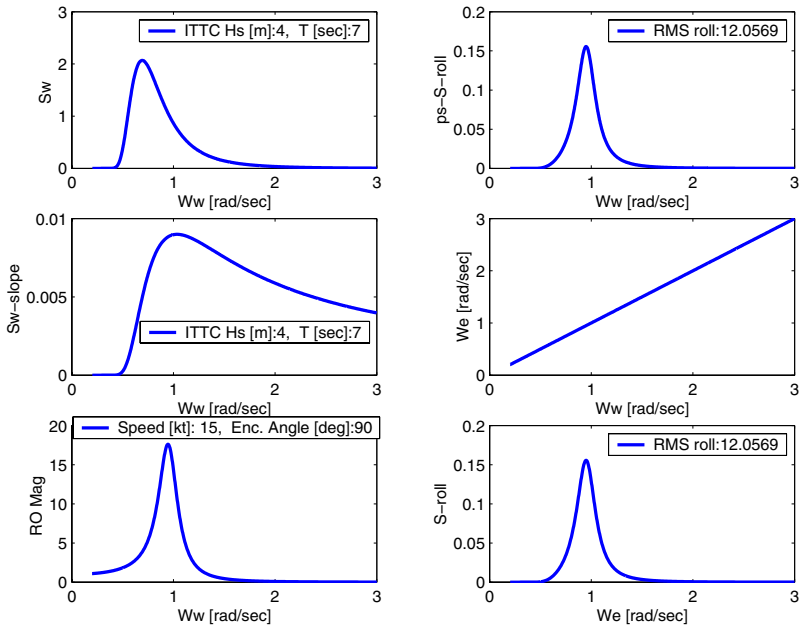

Figure 14.4. Roll motion spectral density used in the simulations.

on the left hand side show the sea elevation spectrum (ITTC spectrum) and

the sea slope spectrum for the adopted sea state. The third plot on the left hand side shows the ship roll response operator from a particular vessel for the adopted sailing conditions (see Perez (2003) for this particular vessel model). The wave slope spectrum is filtered by the hull, and this effect is depicted in the first plot on the right hand side. This plot is called a *pseudo-spectrum* because it is in the wave frequency domain and it is the product of the wave slope spectrum and the roll response operator. The roll power spectral density is finally obtained by transforming the pseudo-spectrum to the encounter frequency domain according to (14.4). This transformation is depicted in the second plot on the right hand side. The roll power spectral density is depicted in the last plot on the right hand side of Figure 14.4.

Once the roll power spectral density has been obtained, the roll motion realisations (time series) can be computed as

$$\phi(t) = \sum_i \bar{\phi}_i \sin(\omega_{ei} t + \theta_i), \tag{14.17}$$

where the phases are chosen randomly with a uniform distribution in $[-\pi, \pi]$ and the amplitudes calculated from

$$\bar{\phi}_i^2 = 2\mathbf{S}_{\phi\phi}(\omega_{ei})\Delta_{\omega i}, \tag{14.18}$$

where $\mathbf{S}_{\phi\phi}(\omega_e)$ represents the roll power spectral density (S-roll in Figure 14.4). The number of regular (sinusoidal) components used to simulate the time series is normally between 500 and 1000 to avoid pattern repetition depending on the total simulation time. This procedure for simulating time series for a ship response is a standard practice in naval architecture and marine engineering; see, for example, Faltinsen (1990).

The measurements taken from one of the realisations were used to estimate the parameters. Figure 14.5 shows the evolution of the estimates of the parameters for the model at a particular sea state and sailing condition. A sampling period of 0.25 sec was adopted based on the value of the roll natural period of the vessel (approximately 7 sec). Finally, Figure 14.6, shows the roll angle and roll rate predictions for two other different realisations using 5 and 10 step-ahead predictions. This consists of using the measured state as initial condition for the model (14.3) with the noises set to their mean values and then running this model forward in time.

From the above example we can see that the filter converges relatively quickly, and the quality of predictions for the behaviour of the ship can be deemed satisfactory. We note that, for the chosen sailing conditions, the use of a second order disturbance model seems to give good results. For other sea conditions, it may be necessary to resort to higher order models, but this shall not be considered here.

This process should be performed before closing the control loop. Then, the proposed control strategy can be considered a quasiadaptive control strategy. That is, if the sailing condition (heading and speed) or the sea state changes,

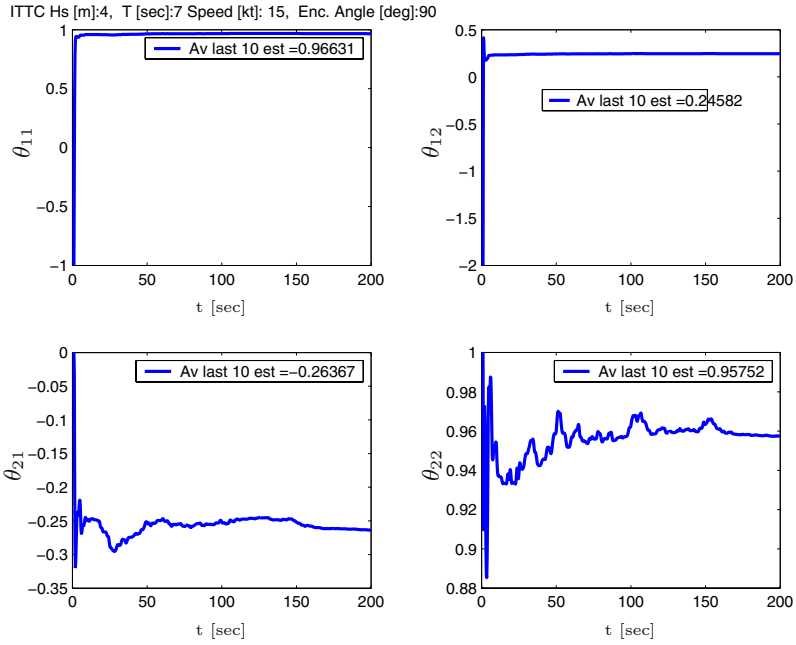

Figure 14.5. Estimated parameters for beam seas.

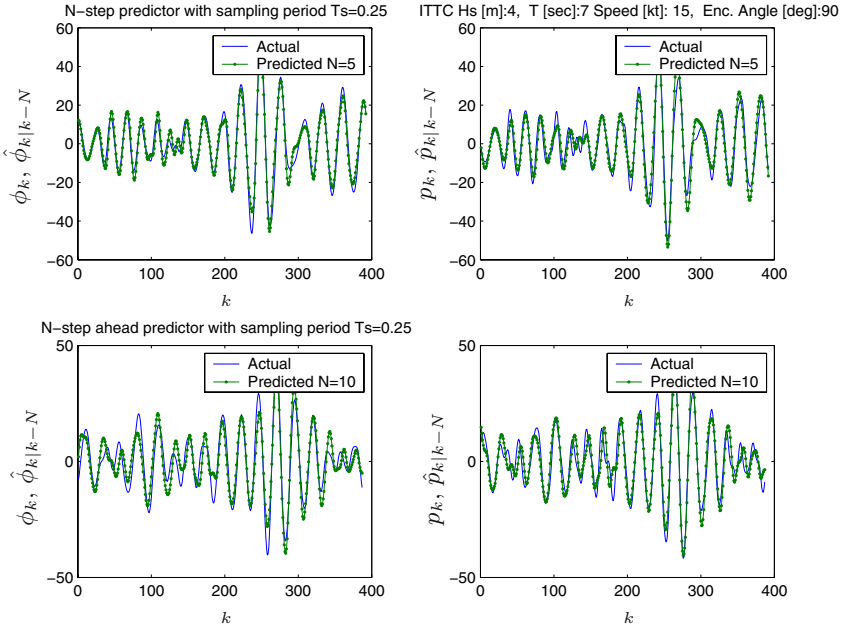

Figure 14.6. Roll angle and roll rate predictions in beam seas.

it may be necessary to open the loop and re-estimate the parameters of the disturbance model to avoid significant degradation in the closed loop performance.

14.8 Constrained Predictive Control of Rudder-Based Stabilisers

In this section, we will present simulation results aimed at assessing the performance of a rudder-based stabiliser designed according to the proposed strategy. In our simulations we will use as a ship a high fidelity nonlinear (calibration) model of a naval vessel adapted from Blanke and Christensen (1993). This model is a very comprehensive model that includes features that are not captured by the simple model used for control system design. However, these features have a direct bearing on the ship dynamic response description. In this fashion, we preserve the degree of uncertainty present in the real application. For the complete model see Perez (2003).

We have selected a speed of 15 kts for the simulations. This is the nominal speed of the vessel and also the speed at which this vessel performs its missions most of the time. The performance will be assessed for the following scenarios:

- **Case A**: Beam seas ($\chi = 90$ deg), $H_s = 2.5$ m, $T = 7.5$ sec;
- **Case B**: Quartering seas ($\chi = 45$ deg), $H_s = 2.5$ m $T = 7.5$ sec;
- **Case C**: Bow seas ($\chi = 135$ deg), $H_s = 4$ m, $T = 9.5$ sec.

The wave heights (H_s) have been chosen to represent moderate and rough conditions under which a vessel the size of this naval vessel can be expected to perform. The particular wave average periods T are the most probable periods for the chosen wave heights in ocean areas around Australia (Perez 2003). The control action will be updated with a sampling rate of 0.25 sec. Finally, the maximum rudder angle will be limited to 25 deg, and maximum rudder rate will be limited to 20 deg/sec.

We will assess the performance via

(i) percentage of reduction in roll angle variance and RMS value;
(ii) yaw angle RMS value induced by the rudder;
(iii) percentage of reduction of motion induced interruptions [MII].

MII is an index that depends on the roll angle and roll acceleration and yields the number of interruptions per minute that a worker can expect due to tipping and loss of balance. The value of this index depends on the particular location on the ship at which it is evaluated. It is a commonly used index to evaluate ship performance in the marine environment (Graham 1990). We will consider a location 7 m above the vertical centre of gravity [VCG] such that we can neglect the effect of vertical motion on the MII. Thus we can simplify the calculations and consider only roll motion. This location coincides with the rear part of the bridge of the vessel.

14.8.1 Tuning

The tuning was performed in beam seas, and then the parameters of the controller were fixed for the rest of the simulation scenarios. The only part of the controller that changed with each sailing condition was the model for the disturbance, which was estimated prior to closing the loop, as indicated in Section 14.7.

Different prediction horizons were tested. As expected, for short prediction horizons ($N = 1$ and $N = 2$), the performance was poorer than for longer horizons ($N = 5$ and $N = 10$). For a horizon of 10 samples periods, an improvement of 10% in roll reduction was achieved with respect to that obtained with $N = 1$. For horizons longer than 10 sample periods there was no significant improvement. Therefore, this is the horizon that was adopted so as to limit the size of the QP problem.

We next present some simulation results. For each case we present a table with the data calculated from the simulated time series and, also, a plot of the corresponding time series.

Case A: Beam Seas

The data for the case of beam seas are shown in Table 14.2.

```
CASE A. Rudder Roll Stabilisation Simulation Report.
        Perez (2003), 14-Jul-2003.
RHC parameters:
Prediction horizon          ---------------------> 10     samples
Sampling time               ---------------------> 0.25   [sec]
Rudder magnitude constraint ---------------------> 25     [deg]
Rudder rate constraint      ---------------------> 20     [deg/sec]
Controller tuning parameters:
Sp=1000; Qp=0; Qr=1; Qphi=100; Qpsi=1; R=0.25

Sailing Conditions:
Wave spectrum               ----------------------> ITTC
Significant wave height     ----------------------> 2.5    [m]
Average Wave period         ----------------------> 7.5    [sec]
Encounter angle             ----------------------> 90     [deg]

Yaw due to stabiliser (RMS) ----------------------> 1.7283 [deg]
Roll open loop (RMS)        ----------------------> 7.2533 [deg]
Roll closed loop (RMS)      ----------------------> 2.7845 [deg]
Reduction  (RMS)            ----------------------> 61.6111 %
Reduction  (VAR)            ----------------------> 85.2629 %

Motion Induced Interruptions @ bridge (7m above VCG):
MII open loop               -------------------> 4.9124  [per min]
MII closed loop             -------------------> 0.28575 [per min]
Reduction                   -------------------> 94.1831 %
```

Table 14.2. Data from the simulated time series for case A: beam seas.

The time series corresponding to the data in Table 14.2 are shown in Figure 14.7. This case is close to the worst condition that the ship can experience

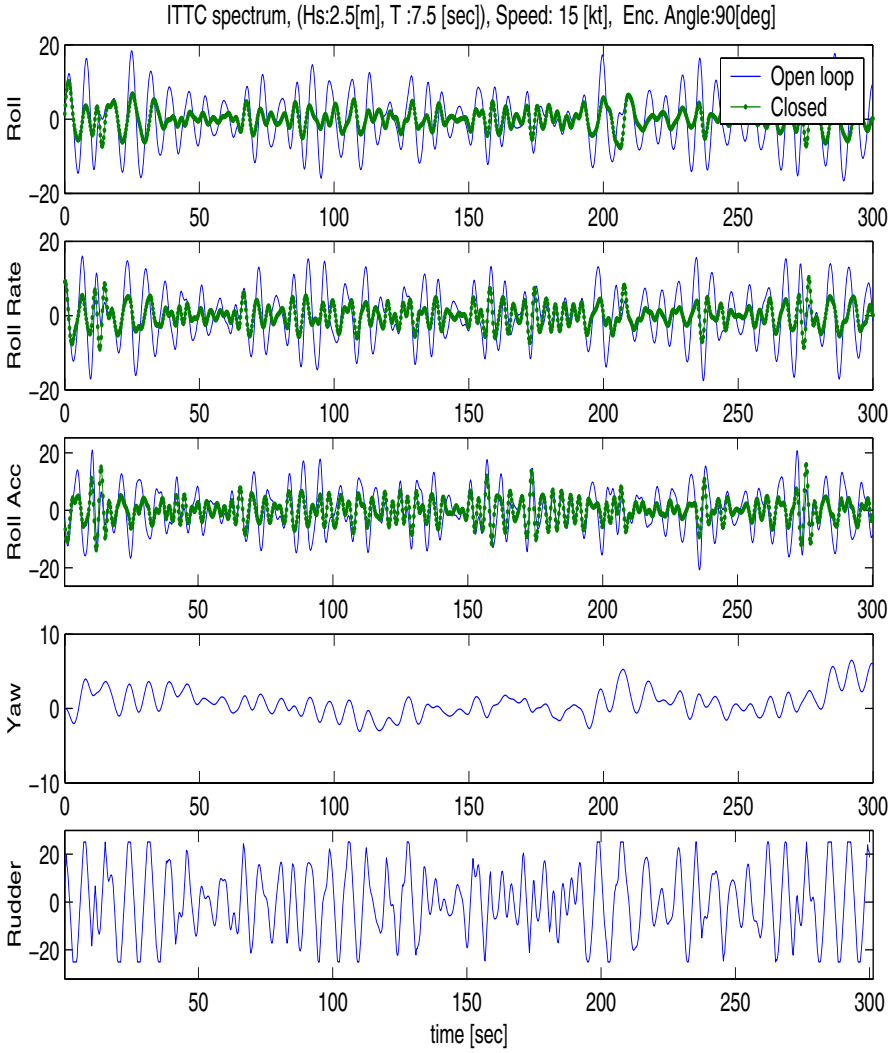

Figure 14.7. Case A. Simulation in beam seas.

in regard to roll motion for the assumed sea state: beam seas. The wave period in this case is close to the natural roll period, which is approximately 7 sec. Therefore, the roll excitation due to the waves is close to resonance. Notwithstanding this, we can still observe good performance.

Results obtained from over 20 different realisations indicate roll reductions on the order of 55–60% for roll RMS values. A significant improvement is achieved, however, in regard to MII: 80–90% reduction.

The inclusion of the term in the objective function that weights roll acceleration $\dot{p}$ yields a smoother control action and a better MII reduction with respect to the case that does not consider this term (between 5–15% higher reduction for the MII), and it yields only a small improvement in the roll angle reduction (less than 5%). This seems to indicate that weighting the roll accelerations in the objective function can be beneficial for operations (missions) that require low MII.

From the rudder action depicted in Figure 14.7, we can see that the controller generates a command that satisfies the magnitude constraints.

Case B: Quartering Seas

The data for the case of quartering seas are shown in Table 14.3.

```
CASE B. Rudder Roll Stabilisation Simulation Report.
        Perez (2003), 14-Jul-2003.
RHC parameters:
Prediction horizon          ---------------------> 10   samples
Sampling time               ---------------------> 0.25 [sec]
Rudder magnitude constraint ---------------------> 25   [deg]
Rudder rate constraint      ---------------------> 20   [deg/sec]
Controller tuning parameters:
Sp= 1000; Qp=0; Qr=1; Qphi=100; Qpsi=1; R=0.25

Sailing Conditions:
Wave spectrum               ---------------------> ITTC
Significant wave height     ---------------------> 2.5   [m]
Average Wave period         ---------------------> 7.5   [sec]
Encounter angle             ---------------------> 45    [deg]

Yaw due to stabiliser (RMS) ---------------------> 6.8057 [deg]
Roll open loop (RMS)        ---------------------> 4.0204 [deg]
Roll closed loop (RMS)      ---------------------> 2.6248 [deg]
Reduction  (RMS)            ---------------------> 34.7126 %
Reduction  (VAR)            ---------------------> 57.3755 %

Motion Induced Interruptions @ bridge (7m above VCG):
MII open loop               -------------------> 0.38515   [per min]
MII closed loop             -------------------> 0.0016905 [per min]
Reduction                   -------------------> 99.5611 %
```

Table 14.3. Data from the simulated time series for case B: quartering seas.

The time series corresponding the data in Table 14.3 are shown in Figure 14.8. The performance in quartering seas decreases significantly. This is expected due to the low encounter frequency of the disturbance. In these conditions, the fundamental limitations associated with the NMP zero and the

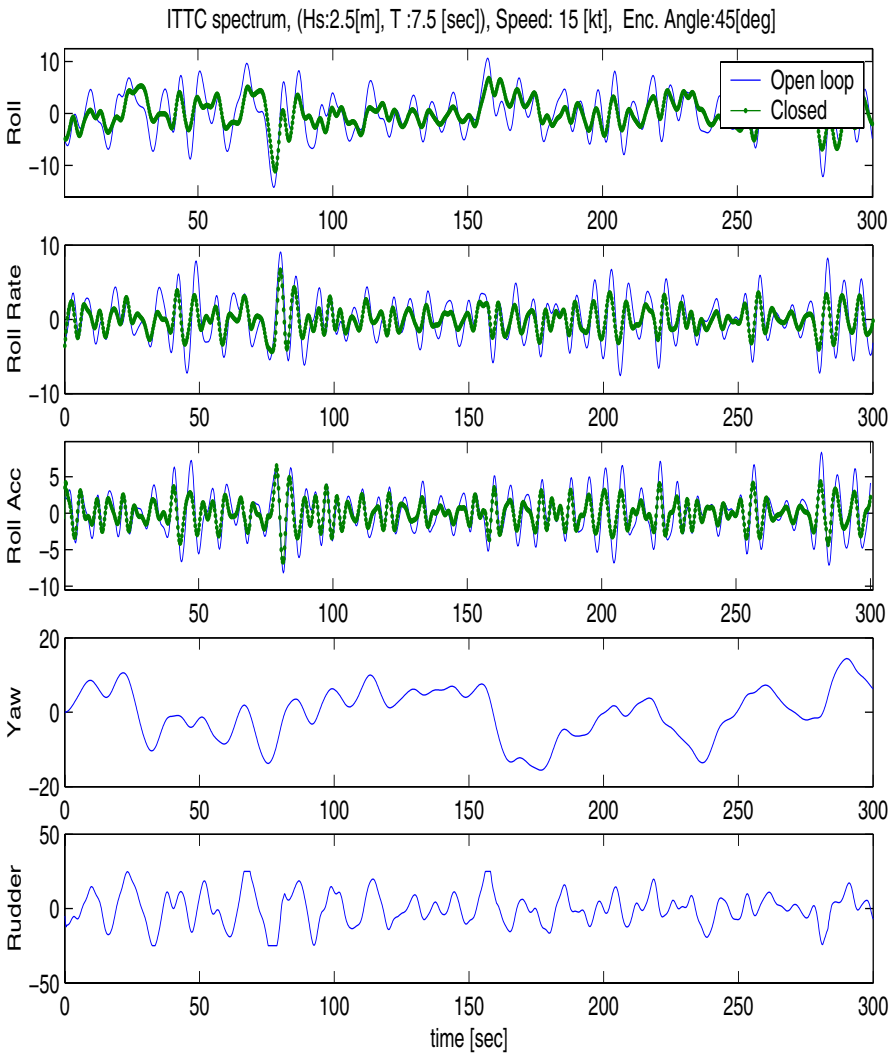

Figure 14.8. Case B. Simulation in quartering seas.

underactuated nature of the system swamp the limitations imposed by the input constraints. Note that the rudder angle depicted in Figure 14.8 rarely hits the constraints. The analysis of the performance in these conditions is beyond the scope of this chapter. The interested reader is encouraged to examine the broader discussion given in Perez, Goodwin and Skelton (2003) and in Perez (2003).

As depicted in Figure 14.8, due to the high interference with yaw for sailing conditions having low encounter frequency, it may be necessary to incorpo-

rate an output constraint in order to limit the maximum heading deviation. The low encounter frequency, here appearing in quartering seas, may also be present in other sailing conditions if the sea state is given by very low period waves produced in severe storms.

Case C: Bow Seas

The data for the case of bow seas are shown in Table 14.4.

```
CASE C. Rudder Roll Stabilisation Simulation Report.
        Perez (2003), 14-Jul-2003.
RHC parameters:
Prediction horizon          ----------------------> 10   samples
Sampling time               ----------------------> 0.25 [sec]
Rudder magnitude constraint ----------------------> 25   [deg]
Rudder rate constraint      ----------------------> 20   [deg/sec]
Controller tuning parameters:
Sp=1000; Qp=0; Qr=1; Qphi=100; Qpsi=1; R=0.25

Sailing Conditions:
Wave spectrum              ----------------------> ITTC
Significant wave height    ----------------------> 4    [m]
Average Wave period        ----------------------> 9.5  [sec]
Encounter angle            ----------------------> 135  [deg]

Yaw due to stabiliser (RMS) ----------------------> 1.1673 [deg]
Roll open loop (RMS)        ----------------------> 4.2398 [deg]
Roll closed loop (RMS)      ----------------------> 1.4856 [deg]
Reduction  (RMS)            ----------------------> 64.9593 %
Reduction  (VAR)            ----------------------> 87.7215 %

Motion Induced Interruptions @ bridge (7m above VCG):
MII open loop               ----------------------> 1.4513 [per min]
MII closed loop             ----------------------> 9.6e-5 [per min]
Reduction                   ----------------------> 99.9934 %
```

Table 14.4. Data from the simulated time series for case C: bow seas.

The time series corresponding the data in Table 14.4 are shown in Figure 14.9. This case presents the best performance despite the more severe sea state: 4 m waves. If we compare the RMS of roll in open loop with that of case B, we can see that these are similar. However, due to the higher encounter frequency of the disturbances in case C, the roll reduction is significantly better. The reason for this is the relative location of the NMP zero (which appears in the response of roll due to rudder) with respect to the bulk of energy of the disturbance (Perez 2003).

14.8.2 The Role of Adaptation

Table 14.5 shows how the adaptation improves the performance of the proposed control strategy for a particular example in which changes in course

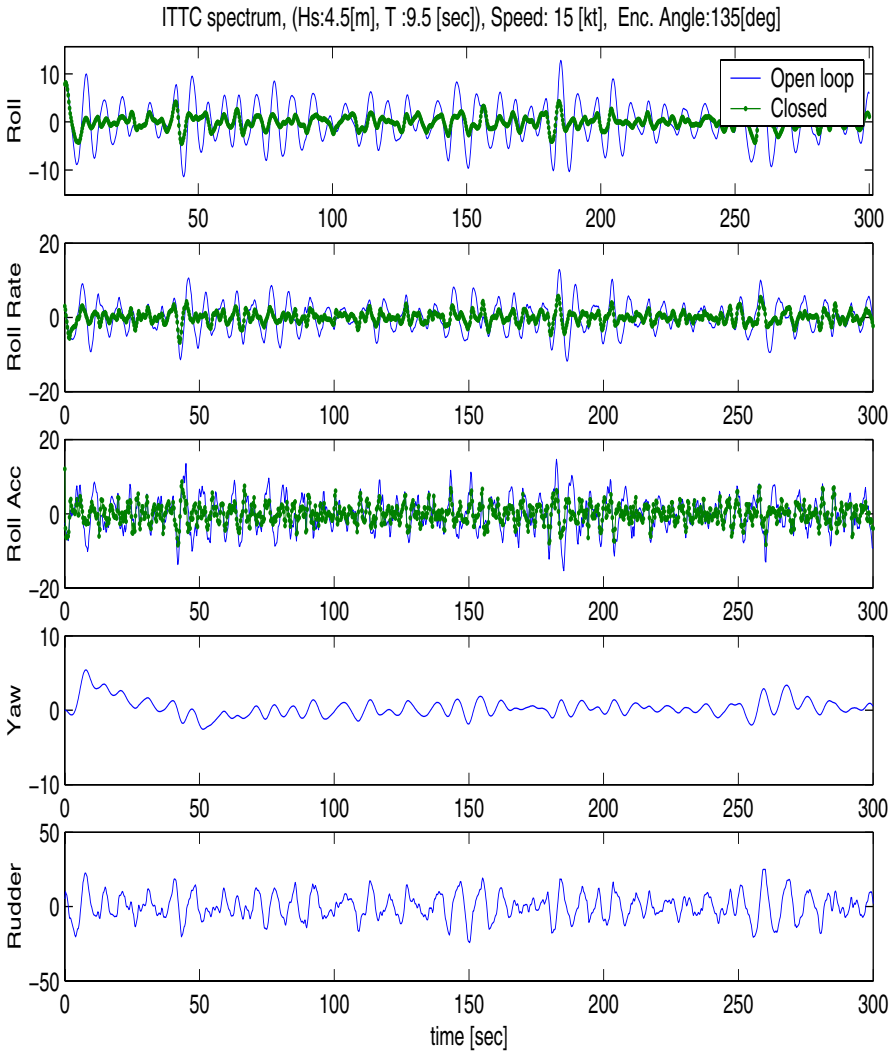

Figure 14.9. Case C. Simulation in bow seas.

from quartering seas to beam seas (χ [deg]: 45→90) and from beam seas to bow seas (χ [deg]: 90→135) were simulated. The second column shows the performance obtained if the disturbance model is not adapted (NA) after the change in course. The third column shows the performance after opening the loop to re-estimate the disturbance model, that is, the model is adapted (A).

We can see a significant improvement in performance due to the adaptation for the course change from quartering to beam seas. However, there is a small improvement for the course change from beam to bow seas. The reason for

this is that the first course change produces more variation in the roll response of the vessel than the second. Therefore, after re-estimating the parameters of the model the performance improves significantly. For the second course change the nonadapted model is still good for the predictions; hence, after adaptation, only a small improvement is obtained.

Although we have only showed, as an illustrative example, variations due to a course change, one should bear in mind that changes in speed and, more importantly, in the sea, determine the characteristics of roll motion. Adaptation plays an important role for the proposed control strategy.

ITTC, Hs=2.5m,T=7.5s	χ [deg]: 45→90 (NA)	χ [deg]: 45→90 (A)
Roll red %	41.5	61.2
MII red %	81.2	99.1
Yaw rms	0.70	0.86
Rudder rms	6.2	10.1
ITTC, Hs=2.5m,T=7.5s	χ [deg]: 90→135 (NA)	χ [deg]: 90→135 (A)
Roll red %	62.0	66. 4
MII red %	100	100
Yaw rms	0.33	0.4
Rudder rms	4.2	5.2

Table 14.5. Performance after a change in course from quartering to beam seas (χ [deg]: 45→90) and from beam to bow seas (χ [deg]: 90→135) with no adaptation (NA) and after adapting the disturbance predictor (A).

14.9 Summary and Discussion

In this chapter, we have presented a case study and control system design for a problem of significant practical importance. The simplifying assumptions under which we performed the design have been kept to a minimum. Hence, almost all aspects of the design process have been addressed to some degree, including choosing the appropriate model, adopting the type of disturbance description and selecting the performance criteria.

The RHC formulation offers a unified framework to address many of the difficulties associated with the control system design for this particular problem: multivariable nature, constraints, uncertainty, stochastic disturbance rejection. The simulations presented illustrate the performance of RHC and suggest that the methodology should be successful in practical applications.

14.10 Further Reading

For complete list of references cited, see References section at the end of book.

General

Further information on rudder roll stabilisation of ships can be found in, for example, Perez (2003) and van Amerongen, van der Klugt and van Nauta Lemke (1990).

For more information on ship dynamics and control, see, for example, Fossen (1994) and Fossen (2002).